

The limits and challenges of error field correction for ITER

R. J. Buttery, A. H. Boozer, Y. Q. Liu, J.-K. Park, N. M. Ferraro et al.

Citation: *Phys. Plasmas* **19**, 056111 (2012); doi: 10.1063/1.3694655

View online: <http://dx.doi.org/10.1063/1.3694655>

View Table of Contents: <http://pop.aip.org/resource/1/PHPAEN/v19/i5>

Published by the [American Institute of Physics](#).

Related Articles

Suppressing electron turbulence and triggering internal transport barriers with reversed magnetic shear in the National Spherical Torus Experiment

Phys. Plasmas **19**, 056120 (2012)

Magnetohydrodynamic spin waves in degenerate electron-positron-ion plasmas

Phys. Plasmas **19**, 052101 (2012)

Tripolar vortex formation in dense quantum plasma with ion-temperature-gradients

Phys. Plasmas **19**, 052303 (2012)

Hamiltonian magnetohydrodynamics: Helically symmetric formulation, Casimir invariants, and equilibrium variational principles

Phys. Plasmas **19**, 052102 (2012)

Orbital ferromagnetism and the Chandrasekhar mass-limit

Phys. Plasmas **19**, 052901 (2012)

Additional information on *Phys. Plasmas*

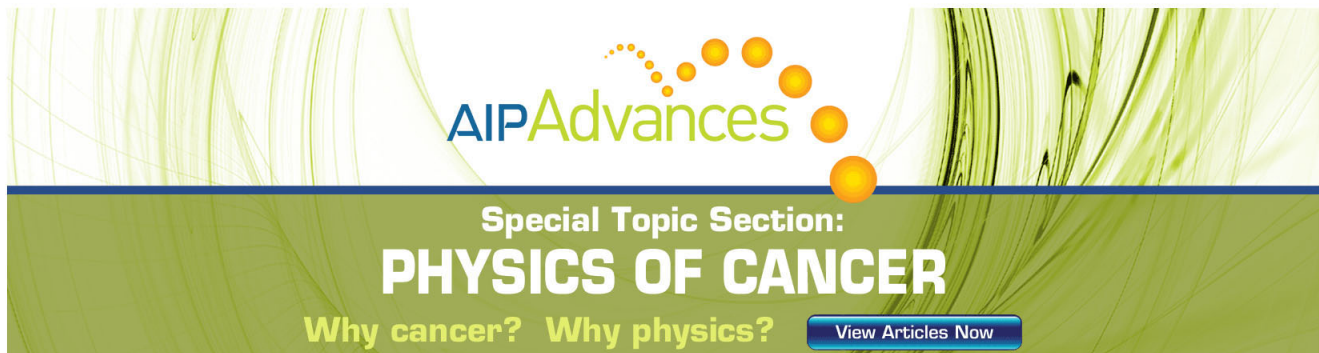
Journal Homepage: <http://pop.aip.org/>

Journal Information: http://pop.aip.org/about/about_the_journal

Top downloads: http://pop.aip.org/features/most_downloaded

Information for Authors: <http://pop.aip.org/authors>

ADVERTISEMENT



AIP Advances

Special Topic Section:
PHYSICS OF CANCER

Why cancer? Why physics? [View Articles Now](#)

The limits and challenges of error field correction for ITER^{a)}

R. J. Buttery,^{1,b)} A. H. Boozer,² Y. Q. Liu,³ J.-K. Park,⁴ N. M. Ferraro,^{1,5} V. Amoskov,⁶ Y. Gribov,⁶ R. J. La Haye,¹ E. Lamzin,⁶ J. E. Menard,⁴ M. J. Schaffer,¹ E. J. Strait,¹ and the DIII-D Team¹

¹General Atomics, P.O. Box 85608, San Diego, California 92186-5608, USA

²Columbia University, New York, New York 10027, USA

³EURATOM/CCFE Fusion Association, Culham Science Centre, Abingdon OX14 3DB, United Kingdom

⁴Princeton Plasma Physics Laboratory, Princeton, New Jersey 08543, USA

⁵Oak Ridge Institute for Science and Education, Oak Ridge, Tennessee 37830, USA

⁶ITER Organization, 13115 St. Paul Lez Durance, France

(Received 20 December 2011; accepted 10 January 2012; published online 29 March 2012)

Significant progress has been made in interpreting the effects of non-axisymmetric “error” fields on a plasma through ideal MHD stability and a dominant “least stable” ideal mode through which the fields couple to the tearing resonant surface. However, in contrast to expectations from such theories, experiments have found limited success in correcting error fields, with single correction coil arrays giving benefits of between 0% and ~50% correction (in terms of improvement to a low density locked mode limit), dependent on the structure of the error and correcting fields. With additional coils up to ~70% is possible. It was unclear whether this represented an intrinsic stability or control limit, or higher order toroidal or poloidal harmonic effects. Thus, studies on the DIII-D tokamak explored correction of a proxy error field, using two differently structured coil arrays. This enabled the principles of error correction to be tested at high amplitudes and operational densities, with known pure $n = 1$ fields. Results showed substantial residual effects from the corrected $n = 1$ field, with improvements of only ~50% in the low density locked mode limit. This suggests that $n = 1$ error fields must couple to more than one surface in the plasma, and this is conjectured to be through more than one ideal mode, thereby requiring precise correction. For ITER, updated predictions of field error have been obtained and compared with revised scalings for tearing mode thresholds, indicating 50% or better error field correction will be needed. This will likely require more than one well coupled correction coil array and sets a challenge for theory to model the behavior, in order to clarify the plasma response and braking mechanisms, and so the effectiveness of ITER’s correction coils and the possible need for support from its edge localized mode control coils. © 2012 American Institute of Physics.

[<http://dx.doi.org/10.1063/1.3694655>]

I. INTRODUCTION

The tokamak is predicated on a toroidally symmetric magnetic field and equilibrium. However, in a real device, small toroidal asymmetries in the magnetic field naturally arise in its design and construction—for example, from the need for current feeds or in construction tolerances. Components of these “error fields” can resonate with surfaces inside the plasma to drive tearing instabilities. This has long been known to pose a concern for tokamak operation and a requirement on its construction tolerances.

In a rotating plasma, resonant error fields are mostly shielded out by image currents at rational surfaces, restricting formation of magnetic islands. However, with finite resistivity, this interaction generates an electromagnetic torque,¹ which changes the phase of the imaging response from perfect shielding to enable slight tearing. Viscous coupling of this tearing structure to the bulk plasma keeps it out of phase with the error field and mostly suppressed, but if the

field is large enough, the electromagnetic torque can overwhelm the rotation leading to a bifurcation to large scale tearing, termed “penetration,” which can ultimately cause a plasma terminating disruption.

These effects pose a particular concern at low plasma density, where decreased viscosity and inertia enable a resonant surface to be slowed more easily, and at low injected torque, which might otherwise help maintain rotation and shielding. They were, therefore, originally considered to be of greatest challenge for ITER during its low density Ohmic phase prior to H-mode access, with the most performance limiting of such tearing modes found to be of 2/1 structure (denoting by *poloidal/toroidal* mode numbers as m/n). On this basis, scalings for error field sensitivity were obtained for ITER,² and an error field correction system designed (Fig. 1).³ This incorporates 3 arrays of field correction coils, in order to be able to independently optimize three $n = 1$ low order poloidal field harmonics ($m = 1, 2, \text{ and } 3$), to allow for toroidal and viscous coupling of harmonics resonant with other rational surfaces on the $q = 2$ surface.

More recently, however, the realization that error fields interact with the plasma through ideal-MHD instabilities⁴⁻⁶ has led to a re-interpretation of their effects. It is now

^{a)}Paper JI2 6, Bull. Am. Phys. Soc. **56**, 137 (2011).

^{b)}Invited speaker. Author to whom correspondence should be addressed. Electronic mail: buttery@fusion.gat.com.

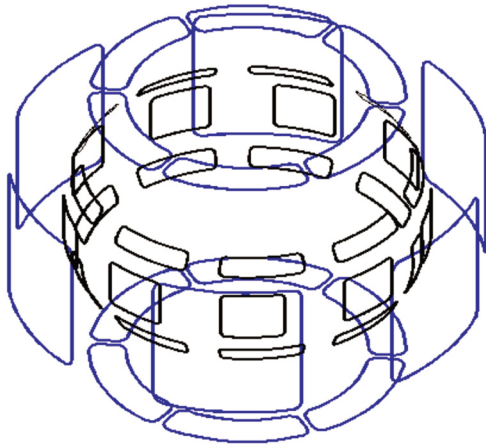


FIG. 1. Schematic of ITER error field correction coils (blue, outer coils) and ELM control coils (black, inner coils), which might, if needed, also be deployed to augment error field correction.

understood that the internal tearing-resonant fields are created in large part from the plasma ideal-MHD response to the error field — in terms of shielding at resonant surfaces, and perturbed currents associated with a driven kink mode distortion. This has mixed implications. On the one hand, it implies an increasing sensitivity to error fields with rises in β , the ratio of thermal to magnetic field energy, as the kink mode becomes more readily driven, amplifying the field inside the plasma.^{5,7} But, it also leads to changes in the spectra of error fields considered to be of greatest concern and, therefore, in the required error field correction strategy. In particular, as the error field is expected to act most strongly through the least stable ideal mode (which generally has weaker pitch than the tearing resonant surface), correction fields tuned to counteract the drive for that mode will have greatest benefit.

Based on these concepts, early work on ideal response^{6,8} suggested a single strongly dominant eigenstructure for coupling external fields to internal tearing resonant fields, and thus, good error field correction in ITER should be quite straightforward by cancelling drive just for this mode.⁸ However, experimental experience has contrasted with this, finding that single coil array correction can have quite limited benefits, highlighting a gap in our understanding. As pointed out in Ref. 9, the limits of error correction will depend on how much and how many secondary ideal MHD modes are driven. It is, therefore, possible (and perhaps likely) that correction to minimize drives for the primary ideal-MHD mode, might increase drives for secondary ideal modes, leading to a residual field in the plasma and braking or coupling through tearing resonant surfaces. Further, the structure of the residual field will govern which types of braking (resonances at various rational surfaces or non-resonant braking through neoclassical toroidal viscosity, “NTV”¹⁰) will apply. Thus, one might envisage suppressing directly resonant 2/1 fields within the plasma, but leaving residual fields elsewhere which might brake rotation and facilitate tearing mode formation.⁷ Therefore, the nature of these braking mechanisms and how they couple through the plasma to lead to tearing modes becomes important, in addition to understanding how

the residual field arises and the strength of the various ideal response modes in the plasma. So far the relative roles and strengths of these effects have not been understood.

Thus, critical questions remain for ITER over the performance of its error correction system (designed for low poloidal mode number vacuum fields), and whether other tools are needed, such as the ELM (edge localized mode) control coils, torque injection, or profile control. As we discuss in Sec. II, threshold scaling and device construction studies indicate that ITER is likely to need significant error field correction. To address how it can go about achieving this, we need to be able to explain existing data in present tokamaks. Thus, in Sec. III, we review the experimental experience with intrinsic error field correction across many devices. This raises a number of questions about what underlies the residual field effects, and these are explored further with experiments using additional coil arrays to explore mitigation of a known proxy error field at much higher amplitude on the DIII-D tokamak (see Sec. IV). The implications of this work for the theoretical understanding, ITER consequences, and further modeling to quantify effects for ITER are discussed in Sec. V.

II. THE ERROR FIELD CHALLENGE FOR ITER

The error field correction system for ITER was originally based on the analysis of low m vacuum-calculated fields, with a criterion based on an empirical approach for Ohmic regimes,² updated for the final ITER design in the papers by Amoskov³ and by Hender.¹¹ Error fields were estimated from a Monte Carlo model of possible error field sources to obtain a prediction of 99% certainty that vacuum calculated resonant fields at the $q = 2$ surface, $\delta B_{2,1}/B_T$, would be no more than 12×10^{-5} (in fact, a 3 mode weighted criterion was used for $m = 1-3$, but we simplify here to the equivalent pure 2/1 field). A demanding target to reduce this measure of error field to 5×10^{-5} was set (and met) for the designed correction system (Fig. 1), giving some margin over the expected threshold of $\sim 12 \times 10^{-5}$ for the fields to trigger locked modes.² However, one should note that the error field components now thought to principally govern the mode formation (in the ideal response formulation) are actually higher in mode number ($m = 7-9$ when computed from the magnetic field pitch at the plasma boundary)⁶ than those calculated in the earlier work—thus, this formalism represents a rather crude estimate of the correction system requirements.

In addition, more recent work¹² has shown error fields pose a greater hazard in H-modes when these are operated at low injected torque (as they will be in ITER). This is of course expected in the ideal response interpretation, as the kink mode becomes more readily driven at the higher β 's of H-modes. Further, in H-mode, the error fields, which act to brake plasma rotation, can often destabilize a rotating 2/1 mode (which locks later), instead of fully arresting rotation to directly drive a locked mode penetration. This is thought to be related to changes in intrinsic tearing mode stability with plasma flow shear.¹³ On this basis, new empirical scalings for mode onset threshold were obtained from DIII-D

(applying a dimensional constraint to infer machine size dependence) for the torque free ITER-baseline-like H-mode in Ref. 12, though with elevated $q_{95} \sim 4.3$, cf. ITERs 3.1 (q_{95} being safety factor at the 95% poloidal flux surface). The metric used to measure field strength was based on calculating applied fields (from the DIII-D I-coils) in terms of the overlap between the field applied at the plasma boundary and the boundary distribution that most efficiently couples (through the ideal plasma response) to generate 2/1 resonant fields at $q = 2$.¹⁴ Using this metric and the empirical scalings, an expected threshold “overlap boundary field,” $\delta B_{\text{overlap}}/B_T$, of 17×10^{-5} was obtained for the ITER baseline. This tolerance for error field in H-mode is some 40% lower than that expected in Ohmic regimes ($\delta B_{\text{overlap}}/B_T = 28 \times 10^{-5}$,¹² if the same metric is applied to the previous Ohmic scalings). It is also seven times lower than the Ohmic scaling prediction when extrapolated to H-mode parameters (where the Ohmic prediction is high, due to the higher density of H-mode). Thus, H-modes are more sensitive to error fields than Ohmic regimes, with thresholds also falling further with rises in β .

These new H-mode scaling extrapolations of error field sensitivity should be compared with expected intrinsic error field levels for ITER, using the same metric. Here, the Monte Carlo simulations have now been updated for the new formalism of overlap field at the plasma boundary.¹⁵ For the ITER baseline burn scenario, this yields individual contributions from sources such as the solenoid, toroidal and poloidal field coils, test blanket modules, etc., in the range $\delta B_{\text{overlap}}/B_T \sim 1\text{--}5 \times 10^{-5}$ each, with an estimated maximum combined total overlap field of $\delta B_{\text{overlap}}/B_T = 28 \times 10^{-5}$. This projection is a mixture of pessimism and optimism. On the one hand, it simply adds up contributions from different sources (assuming they are phase aligned). But on the other hand, within each source of error, such as the PF coil set, it assumes an essentially random distribution of error fields, rather than any systematic trends, in compiling a vector summation to deduce error field.

Thus to stay below the above predicted threshold ($\delta B_{\text{overlap}}/B_T = 17 \times 10^{-5}$ for $q_{95} = 4.3$) would require 40% error field correction. But, if as expected, thresholds fell further for the lower q_{95} of ITER (for example, in line with the Ohmic scaling of $q_{95}^{0.83}$ on DIII-D (Ref. 2)), then correction of 50% will be needed at $\beta_N = 1.8$, and higher for higher β scenarios. This scaling also does not factor in any changes in underlying tearing stability with q_{95} , which are not well known, and it is noted that tearing stability appears to be a significant factor in setting tearing mode limits in H-mode.¹⁶ Thus, significant error field correction on ITER may well be needed, and understanding the relative capabilities of different correction coils is important to determine how to undertake this correction, whether further changes to plasma operation are needed, or if ELM coils are additionally required for error field correction.

III. REVIEW OF PREVIOUS ATTEMPTS AT ERROR FIELD CORRECTION

Error fields or other sources of non-axisymmetric fields have been found to limit operation on several devices

(DIII-D,¹⁷ COMPASS-D and JET,² Alcator C-Mod,¹⁸ MAST,¹⁹ NSTX²⁰). So far, they have tended to pose the greatest problem at low densities in Ohmic operation, and thus particularly as plasmas are started up-H-modes on most devices to date have tended to have high torque and/or plasma rotation, which helps shield out the fields. As a result of the issues in Ohmic plasma, these devices installed perturbative field coils (typically toroidal arrays of near-identical coils to apply a total field with arbitrary toroidal phase and amplitude) to study behavior and develop correction for improved operational access. In all six devices, the fields are found to lead to low density limits in Ohmic regimes which scale close to linearly with the strength of the applied fields. As a result, the density limit can be used to characterize the strength of a device’s intrinsic error field relative to that applied by its perturbative coils and also of the benefits of intrinsic error correction.

Typically, the required correction field is determined by performing a phase scan of fields from the perturbative coils (Fig. 2). Field amplitude is ramped with a given toroidal phase until a mode forms. This is then repeated with other coil phases. Assuming the same total field (intrinsic + applied) at penetration in each discharge enables the deduction of the machine intrinsic error, in terms of equivalent coil currents. Optimal correction is then obtained by applying currents to reach the center of the circle fit to points marking error field threshold (Fig. 2). This approach was confirmed in detailed density ramp-down studies, where a wide variety of correction or error field enhancing currents were applied to discharges in DIII-D to enable fits to identify the optimal correction while confirming linear density scaling of field threshold with total error field.²¹

When applying error field correction, two key observations come to light. First, it is found that the degree of correction obtained, as measured by the improvement in the low

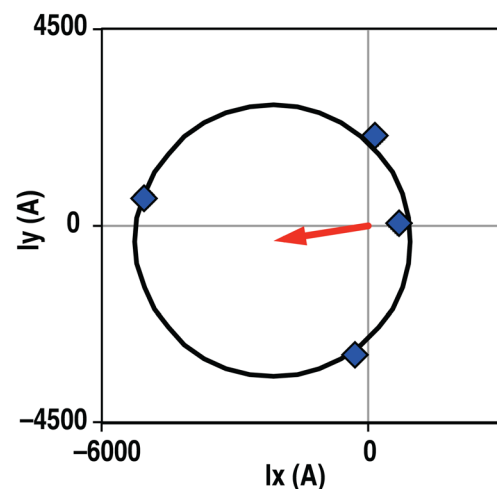


FIG. 2. Measurement of correction field required for an underlying error field. Thresholds for locked modes (diamonds) are measured with field ramps for four phases of the correction coil, plotted here in terms of cosine (I_x) and sine (I_y) components of $n = 1$ array of coil currents. These are fitted by a circle to determine the optimal correction field amplitude and orientation (arrow). (In fact, the error field measured here is the DIII-D C-coil proxy error field source described in Sec. IV using I-coil ramps.)

density locked mode limit, is quite limited. Whilst lower densities can be accessed with error correction, a clear limit is still obtained in how much the density can be reduced without modes, indicative of a substantial residual field effect. Second, the degree of correction obtained is quite variable, dependent on the device and the nature of the coil sets deployed for field measurement and correction. Given the significance of these results, it is worth summarizing them in more detail.

The earliest work came from DIII-D,¹⁷ where it was found that a single “ $n = 1$ ” correction coil located above the plasma (Fig. 3) could enable access to $\sim 25\%$ lower densities. This had limited benefit, perhaps because of the fixed location (i.e., phase) of this single coil. But further work²¹ utilizing an array of ex-vessel midplane “C-coils” showed improvements in density limit of 40%–55%. The degree of benefit, and currents required for optimal correction, depended on the plasma regime and magnetic field structure of the plasma (safety factor, q_{95}). Further, it was found that combining “C-coil” array correction with the $n = 1$ coil led to even better error correction (up to $\sim 70\%$ improvement). This appears to be direct evidence that the correction field’s structure matters in the degree of correction achievable. In the ideal-response interpretation, it also suggests that secondary (and perhaps tertiary) ideal response modes must be playing a significant role, to enable residual fields to couple through the plasma core at significant levels.

The principles of error field correction were established further on DIII-D with the installation of “I-coils,” internal arrays above and below the outboard midplane, which can be flexibly connected to make fields of different pitches.²² Using these internal coils, it was possible to use magnetic feedback to minimize plasma response to an applied C-coil field in high β H-modes,²² thereby providing real time error field correction. Further,²³ it was found that this minimization was most efficient, requiring least coil currents, when the pitch of the I-coil fields was adjusted to match that of the ideal mode (the resistive wall mode) structure. Thus, error correction is best optimized by correcting drive through the least stable ideal mode. Indeed, it was later confirmed that when the correction field structure is most closely aligned to the kink mode structure rather than field line pitch resonance, then this gives the strongest plasma magnetic response to

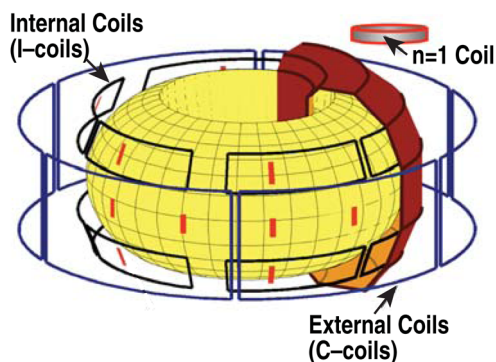


FIG. 3. Coils used in the DIII-D error field experiments: the $n = 1$ coil located on top of the vessel (red), the C-coils on the outside of the vessel (blue), and the internal I-coils (black).

such fields in H-mode and is most effective at triggering a rotation collapse to locked mode.⁷ The I-coils also led to improved density access²⁴ compared to C-coil intrinsic error correction,²¹ confirming that structure of the correction field also influences its effectiveness.

These observations of the variability and limits of error field correction have also been corroborated and extended by other devices. On JET (Ref. 25) internal saddle coils, with toroidal bars located below the plasma either side of the divertor region, led to a 40% reduction in operational density limit when used for error field correction. Crucially, this was good enough correction for tearing modes to unlock, start rotating and decay away. However, when the experiments were repeated with a new coil array,¹⁹ the “error field correction coils” (EFCCs) located ex-vessel on the outboard midplane, the variation in thresholds to induce tearing modes between the different phases of EFCC was found to be negligible, and so no correction improvements were possible (despite there being no known changes made in the underlying JET intrinsic error). The result is interesting because it demonstrates that a coil set, which clearly does couple to the plasma and is able to induce tearing modes (the EFCCs), can generate fields that are effectively orthogonal to another source of field (the machine intrinsic error) that is known to be present on the device. This would appear to indicate more than one mechanism or mode to couple the fields through the plasma and trigger tearing; the two field sources here (intrinsic error and EFCC) must have driven quite different mixes of these response modes. It also highlights the fact that the “wrong” type of correction coil design may offer little benefit for tearing mode avoidance.

In contrast to the JET EFCC results, a similar ex-vessel midplane coil on the spherical tokamak device, MAST, did lead to significant benefits in locked mode density threshold (at least 30%, with no tearing modes found at this density).²⁶ Finally, on C-Mod, a set of two toroidal arrays of four vessel mounted coils, located above and below the midplane (“A-coils”), were found to lead to significant operational improvement, with up to $\sim 60\%$ lower density access.¹⁸ Like the DIII-D I-coils, this seems to confirm that poloidally separated pairs of toroidal coil arrays can be more effective at error correction, perhaps because they are better at canceling out some of the stray harmonics in the plasma and applying a “purer” mix of the right harmonics.

Reviewing this data, it seems clear that correction from a single coil array can achieve anywhere between 0% and 50% improvement in terms of the error field’s effect on locked mode density threshold. The benefits seem to depend on structure of coils and indeed of the plasma and the intrinsic error field, but can be improved further by combining additional coil sets. The results highlight substantial roles associated with residual fields and (in the ideal response interpretation) secondary ideal modes through which the coils couple to the plasma. These observations, all obtained with $n = 1$ coil configurations, indicate that it is likely that $n = 1$ is an important toroidal harmonic to consider. Nevertheless, it is also possible that residual corrected error field effect may come from higher n components. However, the results summarized here are hard to analyze cleanly, because

they all involve relatively poorly known intrinsic error field distributions. They also do not rule out the possibility of other sources of limitation, such as intrinsic instability or control error.

IV. TESTING THE PHYSICS OF ERROR FIELD CORRECTION WITH A KNOWN PROXY FIELD

There has been much speculation over the origins of the limits of error field correction in accessing low density—suggested to arise from unknown field components, additional NTV effects, higher n fields, or even control problems. To explore this in a controlled and modelable manner, dedicated experiments were formulated on DIII-D, using its unique multiple coil arrays (Fig. 3) to generate a proxy $n = 1$ error field with one coil set (the “C-coils”) and then attempt correction with a second array (the “I-coils”). These coil sets have dramatically different field structures (see Fig. 4), as is usually the case in intrinsic error field correction. Thus, experiments could explore correction of a known, large dominant proxy error field with pure $n = 1$ structure.

Discharges were obtained by first ramping the density to a high value to then enable the application of a significant amplitude C-coil proxy field without immediately inducing tearing modes. I-coils were then ramped with various phases relative to the C-coil field to measure the optimal correction field. I-coils were deployed with the usual 240° toroidal phase difference between the upper and lower arrays, found optimal for intrinsic error correction on DIII-D in the standard left-handed magnetic field equilibrium, and best aligned with ideal MHD modes.⁷ A subtlety of the experiment was that the phase scan was performed by rotating the source C-coil proxy field phase (with fixed I-coil phase throughout) rather than the I-coil phase. This meant that the phase scan measured just the proxy field (which was rotated past the sensing I-coil field) and not the machine intrinsic error well. To further reduce uncertainties from machine intrinsic

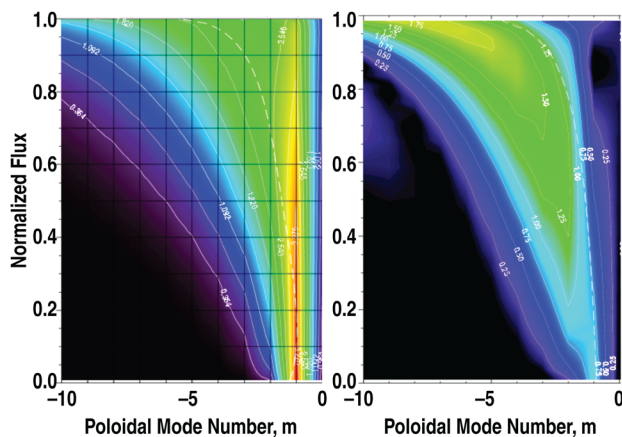


FIG. 4. Comparison of $n = 1$ field spectra of C-coils (left) and I-coils (right): color indicates field strength (arbitrary scales—black-blue-green-red or dark to light for increasing amplitude) for a given poloidal harmonic (x value, negative for relevant plasma helicity) and radial location (y value). The white dashed line indicates q value (read off x axis) for given radius. The C-coils make a much more core localized perturbation, while the I-coils make a field most resonant with higher mode numbers nearer the edge of the plasma.

error field, a phase scan of C-coil current ramps was performed prior to the I-coil experiments, to deduce the C-coil currents that minimize machine error. These were applied as offsets to the C currents used to generate the proxy fields in the main experiment. Finally, in the main experiment, the I-coil phase (which was kept fixed, as noted above) was chosen to be orthogonal to the measured machine error and its correction by the C-coils, in order to minimize the effects of any inaccuracy in the intrinsic error correction optimization (the residual field would be mostly orthogonal to the proxy field).

A typical experiment is shown in Fig. 5. As the density was ramped up, C-coils were applied to correct just the intrinsic machine error. Once high density was reached, C-coils were switched to apply the additional proxy error field with 2 kA peak amplitude and an $n = 1$ sinusoidal distribution in toroidal angle. I-coils were then slowly ramped to determine the level that induces a static tearing mode, as observed by a triplet of toroidally opposite saddle loop detectors. The resulting $n = 1$ I-coil currents at mode penetration are those of Fig. 2, where the vector orientation of points represents the phase of the I-coil field relative to that of the applied C-coil proxy field (taking I-coil phase as the average between the upper and lower coil orientations) for each of four discharges. Fitting with an offset circle, it is found that

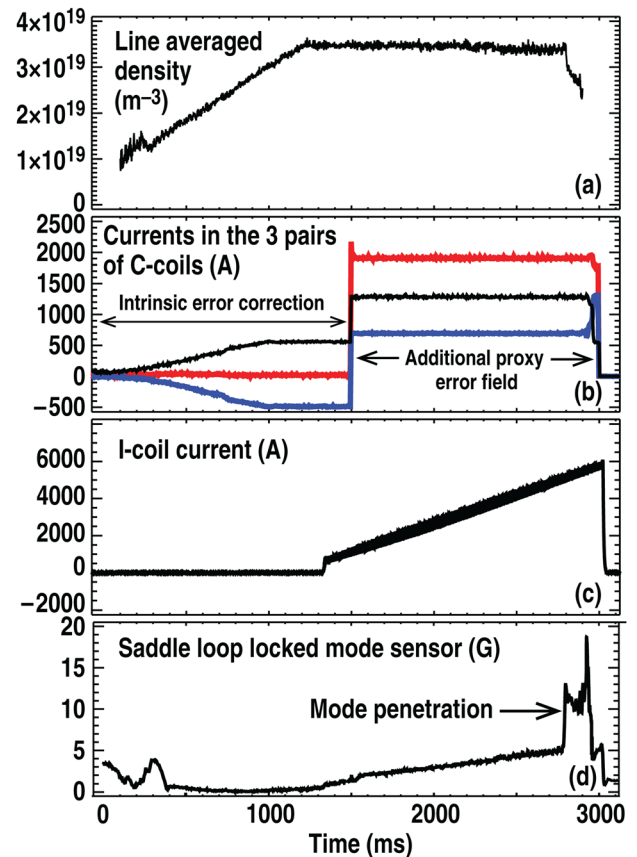


FIG. 5. Example of proxy error field experiments: (a) density is ramped up, (b) currents in 3 toroidally opposite pairs of C-coils are deployed first to correct the intrinsic error field and then apply a larger proxy error field, (c) I-coil currents are then ramped (in 3 pairs, only one shown) to a trigger a mode, and (d) mode formation (“penetration”) observed on locked mode sensor.

optimal correction of the proxy error is obtained with 2.2 kA amplitude currents in the I-coils, and at a phase of 171° —close to perfect opposition to the C-coil proxy field (a small difference might be expected as fields are structured differently and so might couple differently to the plasma; there is also a natural scatter in the data). This I-coil correction field was then applied to density ramp-downs with proxy field still deployed, to determine the benefits of correction in terms of locked mode density limits, as shown in Fig. 6.

Before considering the implications of these results, it is important to consider the influence of the machine intrinsic error: to obtain relevant results from these experiments, sufficient headroom in density had to be generated to enable the application of the proxy field and optimization of its correction at levels well above those associated with the corrected intrinsic error. However, density had to be low enough to avoid I-coil currents in the phase scan exceeding power supply limits (6.3 kA). The parameter space is summarized in Fig. 7. Considering first the underlying intrinsic error, the density ramp-down in discharge 144 428 captures the locked mode threshold with uncorrected intrinsic error field, $0.95 \times 10^{19} \text{ m}^{-3}$. However, with re-optimized intrinsic error correction from the C-coils, this was reduced to $0.44 \times 10^{19} \text{ m}^{-3}$ —a good level of correction. This re-optimized correction, required currents of up to 500 A in the C-coils, and this was used as the basis for the proxy field studies. The choice of 2 kA of applied C-coil proxy field enabled this to dominate over intrinsic error. Combined with an operational density of $\sim 3.4 \times 10^{19} \text{ m}^{-3}$ in the phase scan, this gave sufficient head-

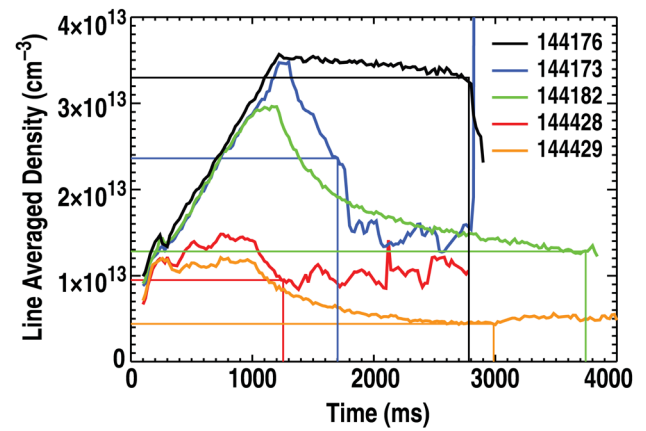


FIG. 7. Operational space of proxy error field experiment, with mode onset times and densities marked by correspondingly colored straight lines. In order of decreasing locked mode density: constant density discharge with proxy field and I-coil ramp (black, 144 176), density ramp-downs with proxy field applied (blue, 144 173), I-coil-corrected proxy field (green, 144 182), machine error only (red, 144 428), and C-coil-corrected machine error (orange, 144 429).

room to trigger mode formation in all phases of the scan. The dominance of the proxy field over the corrected intrinsic error field is indicated by the density access limits in Fig. 7; the density ramp-down with the proxy field applied led to a density limit of $2.46 \times 10^{19} \text{ m}^{-3}$ (this number based on averaging two discharges)—well above corrected intrinsic error limits. Further, using I-coils to correct this proxy field, lowered the density limit to $1.28 \times 10^{19} \text{ m}^{-3}$ —still substantially higher than the corrected intrinsic error field which gave a locked mode density threshold of $0.44 \times 10^{19} \text{ m}^{-3}$.

This corrected proxy field density limit is substantially larger than might arise simply from the scatter in the phase scan analysis of Fig. 2, which might lead to inaccuracies in the optimal correction field, and so less good correction. Here, the standard deviation in currents from the circular fit is 190 A, which translates to the same sized error bar in the precision of the correction itself. Taking a worst case of assuming the impact on density limit scales proportionately from the $2.46 \times 10^{19} \text{ m}^{-3}$ density limit obtained with the pure proxy field, which required 2.2 kA of I-coil current to correct, the error bar in density limit is found to be $\pm 0.2 \times 10^{19} \text{ m}^{-3}$, which is only 17% of the corrected proxy field density limit ($1.28 \times 10^{19} \text{ m}^{-3}$). Thus, provided optimal correction does indeed occur at the center of the circle fit (as implicitly confirmed in Ref. 21), then the corrected proxy density limit must substantially arise from residual fields with optimized correction rather than an inaccurate optimization of the correction itself. Of course, given more experiment time, it would be desirable to confirm this point directly, by checking that there was not a nearby correction phase and amplitude that could lower the density limit further.

A further uncertainty might arise from the time taken for the applied field to trigger a mode, as the plasma takes time to brake before reaching the bifurcation to penetration. Here, we have assumed there is a torque balance equilibrium maintained throughout, so modes form as soon as the field is large enough for this torque balance to be overcome. However, if

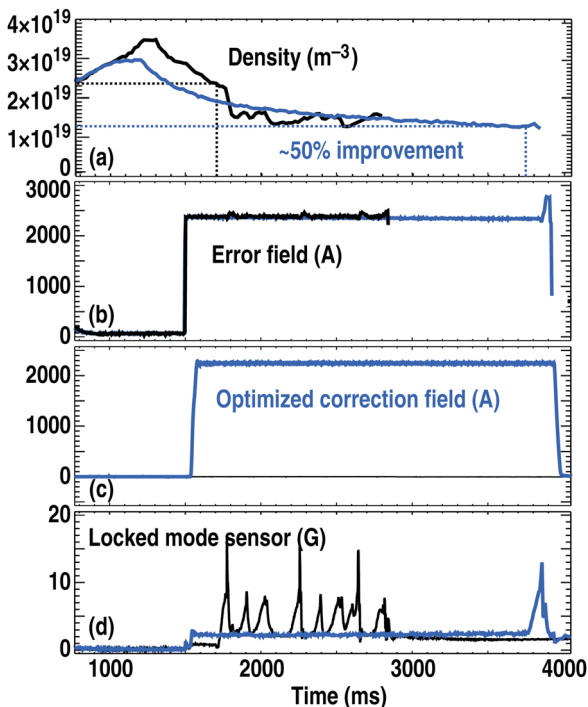


FIG. 6. Benefits of proxy error field correction measured by density ramp-down: (a) density is first ramped up, enabling (b) proxy field to be applied without causing a mode, and is then ramped down to measure density limit observed via locked mode onset (d). In first shot (black, 144 173, which terminates early), only C-coils are applied, and in second shot (blue, 144 182, which runs full length), I-coil currents are applied (c) as deduced in Fig. 2 to correct out proxy field.

there is a characteristic timescale for the plasma rotation to respond to changes in 3D field, then there may be a slight delay. Estimating this as comparable to the energy (in lieu of momentum) confinement timescale (typically 50 ms in Ohmic plasmas²⁷), and considering the I-coil ramp-rates yields an error bar in optimal correction currents ± 60 A, or about $\pm 0.07 \times 10^{19} \text{ m}^{-3}$ in terms of density limit impact using arguments as in the previous paragraph—a modest effect.

Thus, the analysis indicates that optimal I-coil correction of the proxy field still leaves a substantial mode-inducing residual field, considerably larger than the corrected intrinsic error. This residual field must have an $n = 1$ structure— $n = 0, 2, 3, 4,$ and 6 fields are eliminated as an origin of observed limits, as these are negligible thanks the six-fold symmetry of the I- and C-coils deployed (any components of these other n fields generated by one coil, will be cancelled by an opposite field component from the other coils).

Finally, to better quantify the degree of proxy field correction obtained, one needs to allow for the residual corrected intrinsic field. This can be estimated by using density thresholds as a measure of field amplitude (noting the linear relation generally observed). If one considers that the proxy field was applied at 90° to the intrinsic error and their correction fields and also that it is likely comprised of a different harmonic mix, it would seem reasonable to consider the C-coil corrected intrinsic error field and proxy fields to be reasonably orthogonal—both in harmonic content and orientation of any common harmonics. Thus, the total field leading to a locked mode can be considered as the sum of these two components added in quadrature, as discussed in Ref. 12. Recalling the proportional relationship generally observed between locking density and perturbation field amplitude gives the expected density limit from the underlying corrected proxy field (excluding contribution from corrected intrinsic error) as $\sqrt{(1.28^2 - 0.44^2)} = 1.20 \times 10^{19} \text{ m}^{-3}$, compared to that of the uncorrected proxy field (also excluding contribution from corrected intrinsic error) of $2.42 \times 10^{19} \text{ m}^{-3}$. Thus, the correction field has removed $\sim 50\%$ of the operational effect of the proxy field—a strong $n = 1$ field remains that couples through the plasma to induce a tearing mode.

V. DISCUSSION

The obvious question arising from these observations is “what do they imply for the mechanisms by which error fields couple to the plasma?” The proxy experiment confirms that the residual field effects are strong manifestations of the error field physics—not control or operational limits from other processes and also not solely arising from higher n components (though these could in principle pose additional challenges). They show that, even for pure $n = 1$ fields, the correction is limited with a single fixed field structure coil array (here to the $\sim 50\%$ level in terms of density limit benefit).

In the ideal response interpretation, this indicates that the fields are likely to couple to the plasma through more than a single “least stable” ideal mode—perhaps, either a secondary ideal mode of similar response (i.e., stability) to the first or a

number of weaker ideal modes that add up to the same effect. Further, the resultant internal fields must act on the plasma through more than one resonant surface—a single surface resonant response would be entirely cancellable with appropriate adjustment of amplitude and phase of a single array of correction coil currents, irrespective of through which ideal modes they couple. Thus, the resulting variation in internal field structure when error field correction is deployed, might lead to the variations in the degree of braking and triggering of modes in the plasma. For example, peaks in fields might form at locations that generate more braking or lead more readily to tearing. The challenge now lies in explaining the strength of the plasma ideal response, where these residual fields lie in the plasma and what sorts of braking the fields might lead to. This is naturally a task that can be further advanced using the modeling tools described earlier in this paper, constructing cases of proxy field correction, looking at the strength of the ideal plasma response, and calculating the various types of braking (resonant at various surfaces and NTV braking) to explore these possibilities and identify the significant sources of interaction.

Nevertheless, further clues can be gleaned from the wider experience of error correction. The limitations in single array correction corroborate a strong role of residual fields, possible secondary ideal mode responses, and significant interaction through more than one surface in the plasma. Indeed, even with two sets of correction coils, DIII-D found limited benefits, hinting that further (tertiary) ideal modes may play a role or, simply, that it is not that easy to null out fields in the plasma. It is therefore possible and perhaps likely that as correction fields are used to null out drives for the dominant ideal mode and resonant responses, this may drive the combinations of higher order of ideal modes that lead to localized increases in fields elsewhere. In this situation, effects such as NTV, which are volume integral and additive, may play a stronger role. This will lead to needs for multiple coil array correction. Perhaps the most interesting result is the lack of effective correction with EFCCs on JET—where despite these coils being able to couple to the plasma and readily trigger tearing modes, they had almost no operational benefit for intrinsic error correction and seemed to act entirely orthogonally to the JET intrinsic error field. This is a strong indicator that more than one mechanism or mode may exist through which the fields can couple to the plasma.

For ITER, these limits suggest that it will need to deploy more than one correction coil set, unless behavior is favorably impacted by an anomalous strong rotation source. It also shows that the shape of the coil set (and intrinsic error) matters. Without a full understanding of the effects described here, it is impossible to make hard numerical predictions of the effectiveness of its correction systems. Nevertheless, one might empirically conclude as follows: ITERs midplane coils offer significant potential for correction of error field magnitude, possibly by as much as a $\sim 50\%$ reduction, as observed with the DIII-D C-coils impact on density limit. However, the level of benefit will depend on the exact nature of the underlying error field. If the midplane coils turn out to be not well aligned with the intrinsic error for its correction

(as has been observed on JET with the EFCC coils), then the top and bottom coils are likely to provide important further harmonic flexibility. Thus, a 50% benefit from the full ITER correction system looks a reasonable objective, though progress beyond the 50% level seems more speculative, as these coils are poorly located for resonance with the kink instability. This 50% correction appears to be close to what will be needed, when the latest predictions for error field sensitivity for ITER H-modes¹² are compared with updated estimates for actual intrinsic error field levels expected in ITER.¹⁵ However, with uncertainties in the degree of correction possible, the q_{95} dependence and desire for a wider operational range in β_N , it is desirable to have some further margin. This looks likely to be possible to provide with the ELM control coils, which have the proximity and flexibility to do significantly better correction, noting the benefits of coil pairs and/or coils close to the plasma on DIII-D, C-Mod, and JET. Thus, for the time being, ITER should retain the option to deploy error field correction with its ELM control coils. It is now incumbent on the community to understand these processes better and put this correction on a firmer footing.

ACKNOWLEDGMENTS

This work was supported in part by the U.S. Department of Energy under DE-FC02-04ER54698, DE-FG02-04ER54761, DE-AC02-09CH11466, and DE-AC05-06OR23100.

- ¹R. Fitzpatrick and T. C. Hender, *Phys. Fluids B* **3**, 644 (1991).
- ²R. J. Buttery, M. De'Benedetti, D. A. Gates, Yu. Gribov, T. C. Hender, R. J. La Haye, P. Leahy, J. A. Leuer, A. W. Morris, A. Santagiustina, J. T. Scoville, B. J. D. Tubbing, JET Team, COMPASS-D Research Team, and DIII-D Team, *Nucl. Fusion* **39**, 1827 (1999).
- ³V. Amoskov, A. Belov, V. Belyakov, O. Filatov, Yu. Gribov, E. Lamzin, N. Maximenkova, B. Mingalev, and S. Sytchevsky, *Plasma Devices Oper.* **13**, 87 (2005).
- ⁴A. H. Boozer, *Phys. Rev. Lett.* **86**, 5059 (2001).
- ⁵A. M. Garofalo, T. H. Jensen, L. C. Johnson, R. J. La Haye, G. A. Navratil, M. Okabayashi, J. T. Scoville, E. J. Strait, D. R. Baker, J. Bialek, M. S. Chu, J. R. Ferron, J. Jayakumar, L. L. Lao, M. A. Makowski, H. Reimerdes, T. S. Taylor, A. D. Turnbull, M. R. Wade, and S. K. Wong, *Phys. Plasmas* **9**, 1997 (2002).
- ⁶J.-K. Park, M. J. Schaffer, J. E. Menard, and A. H. Boozer, *Phys. Rev. Lett.* **99**, 195003 (2007).
- ⁷H. Reimerdes, A. M. Garofalo, E. J. Strait, R. J. Buttery, M. S. Chu, Y. In, G. L. Jackson, R. J. La Haye, M. J. Lanctot, Y. Q. Liu, M. Okabayashi, J.-K. Park, M. J. Schaffer, and W. M. Solomon, *Nucl. Fusion* **49**, 115001 (2009).
- ⁸J.-K. Park, A. H. Boozer, J. E. Menard, and M. J. Schaffer, *Nucl. Fusion* **48**, 045006 (2008).
- ⁹A. H. Boozer, *Fusion. Sci. Technol.* **59**, 561 (2011).
- ¹⁰K. C. Shaing, *Phys. Rev. Lett.* **87**, 245003 (2001).
- ¹¹T. C. Hender, J. C. Wesley, J. Bialek, A. Bondeson, A. H. Boozer, R. J. Buttery, A. Garofalo, T. P. Goodman, R. S. Granetz, Y. Gribov, O. Gruber, M. Gryaznevich, G. Giruzzi, S. Günter, N. Hayashi, P. Helander, C. C. Hegna, D. F. Howell, D. A. Humphreys, G. T. A. Huysmans, A. W. Hyatt, A. Isayama, S. C. Jardin, Y. Kawano, A. Kellman, C. Kessel, H. R. Koslowski, R. J. La Haye, E. Lazzaro, Y. Q. Liu, V. Lukash, J. Manickam, S. Medvedev, V. Mertens, S. V. Mirnov, Y. Nakamura, G. Navratil, M. Okabayashi, T. Ozeki, R. Paccagnella, G. Pautasso, F. Porcelli, V. D. Pustovitov, V. Riccardo, M. Sato, O. Sauter, M. J. Schaffer, M. Shimada, P. Sonato, E. J. Strait, M. Sugihara, M. Takechi, A. D. Turnbull, E. Westerhof, D. G. Whyte, R. Yoshino, H. Zohm, and the ITPA MHD, Disruption, and Magnetic Control Topical Group, *Nucl. Fusion* **47**, S128 (2008).
- ¹²R. J. Buttery, S. Gerhardt, R. J. La Haye, Y. Q. Liu, H. Reimerdes, S. Sabbagh, M. S. Chu, T. H. Osborne, J.-K. Park, R. I. Pinsker, E. J. Strait, J. H. Yu, and the DIII-D and NSTX Teams, *Nucl. Fusion* **51**, 073016 (2011).
- ¹³R. J. La Haye, D. P. Brennan, R. J. Buttery, and S. P. Gerhardt, *Phys. Plasmas* **17**, 056110 (2010).
- ¹⁴J.-K. Park, J. E. Menard, M. J. Schaffer, H. Reimerdes, A. H. Boozer, R. J. Buttery, C. M. Greenfield, D. A. Gates, S. P. Gerhardt, R. J. La Haye, R. M. Nazikan, S. A. Sabbagh, J. A. Snipes, J. T. Scoville, S. M. Wolfe, the NSTX Research Team, the DIII-D Research Team, and the TBM International Research Team, in *Proceedings of the 23rd Fusion Energy Conference, Daejeon, Korea, 2010* (IAEA, Vienna, 2010), EXS/P5-12.
- ¹⁵Y. Gribov, "Error fields expected in ITER and their correction," ITER Report ITER_D_4GKRYC (version 1.1), ITER Organization, France, 15 June 2011.
- ¹⁶R. J. Buttery, R. J. La Haye, P. Gohil, G. L. Jackson, H. Reimerdes, E. J. Strait, and the DIII-D Team, *Phys. Plasmas* **15**, 056115 (2008).
- ¹⁷J. T. Scoville, R. J. La Haye, A. G. Kellman, T. H. Osborne, R. D. Stambaugh, E. J. Strait and T. S. Taylor, *Nucl. Fusion* **31**, 875 (1991).
- ¹⁸S. M. Wolfe, I. H. Hutchinson, R. S. Granetz, J. Rice, A. Hubbard, A. Lynn, P. Phillips, T. C. Hender, D. F. Howell, R. J. La Haye, and J. T. Scoville, *Phys. Plasmas* **12**, 056110 (2005).
- ¹⁹D. F. Howell, T. C. Hender, R. J. La Haye, J. T. Scoville, S. Wolfe, and I. Hutchinson, "Machine size scaling of error field induced locked mode thresholds," *Bull. Am. Phys. Soc.* **49**, 76 (2004).
- ²⁰J. E. Menard, R. E. Bell, D. A. Gates, S. P. Gerhardt, J.-K. Park, S. A. Sabbagh, J. W. Berkery, A. Egan, J. Kallman, S. M. Kaye, B. LeBlanc, Y. Q. Liu, A. Sontag, D. Swanson, H. Yuh, W. Zhu, and the NSTX Research Team, *Nucl. Fusion* **50**, 045008 (2010).
- ²¹J. T. Scoville and R. J. La Haye, *Nucl. Fusion* **43**, 250 (2003).
- ²²G. L. Jackson, P. M. Anderson, J. Bialek, W. P. Cary, G. L. Campbell, A. M. Garofalo, R. Hatcher, A. G. Kellman, R. J. La Haye, A. Nagy, G. A. Navratil, M. Okabayashi, C. J. Pawley, H. Reimerdes, J. T. Scoville, E. J. Strait, and D. D. Szymanski, in *Proceedings of 30th EPS Conference, St. Petersburg, ECA*, St. Petersburg, Mulhouse, France (European Physical Society, 2003), Vol. 27A, p. 4.47.
- ²³E. J. Strait, J. M. Bialek, I. N. Bogatu, M. S. Chance, M. S. Chu, D. H. Edgell, A. M. Garofalo, G. L. Jackson, R. J. Jayakumar, T. H. Jensen, O. Katsuro-Hopkins, J. S. Kim, R. J. La Haye, L. L. Lao, M. A. Makowski, G. A. Navratil, M. Okabayashi, H. Reimerdes, J. T. Scoville, A. D. Turnbull, and DIII-D Team, *Phys. Plasmas* **11**, 2505 (2004).
- ²⁴J.-K. Park, M. J. Schaffer, R. J. La Haye, T. J. Scoville, and J. E. Menard, *Nucl. Fusion* **51**, 023003 (2011).
- ²⁵R. J. Buttery, M. De'Benedetti, T. C. Hender, and B. J. D. Tubbing, *Nucl. Fusion* **40**, 807 (2000).
- ²⁶D. F. Howell, T. C. Hender, and G. Cunningham, *Nucl. Fusion* **47**, 1336 (2007).
- ²⁷D. P. Schissel, A. G. Kellman, R. T. Snider, R. D. Stambaugh, K. H. Burrell, J. C. DeBoo, T. H. Osborne, J. D. Callen, and Z. Chang, *Nucl. Fusion* **32**, 107 (1992).